Received: 19 February 2024 | Revised: 31 July 2024 | Accepted: 4 September 2024

DOI: 10.1111/jne.13450

ORIGINAL ARTICLE

Journal of Neuroendocrinology WILEY

Rapid and local neuroestrogen synthesis supports long-term potentiation of hippocampal Schaffer collaterals-cornu ammonis 1 synapse in ovariectomized mice

Matthieu J. Maroteaux[1,2] | Claire T. Noccioli[1,2] | Jill M. Daniel[1,2] | Laura A. Schrader[2,3]

[1]Department of Psychology, Tulane University, New Orleans, LA, USA

[2]Tulane Brain Institute, Tulane University, New Orleans, LA, USA

[3]Department of Cell and Molecular Biology, Tulane University, New Orleans, LA, USA

Correspondence
Matthieu J. Maroteaux, Psychology, Tulane University, 6400 Freret St., New Orleans, LA, 70118, USA.
Email: mmaroteaux@tulane.edu

Funding information
National Institute on Aging, Grant/Award Number: RF1AG041374

Abstract

In aging women, cognitive decline and increased risk of dementia have been associated with the cessation of ovarian hormones production at menopause. In the brain, presence of the key enzyme aromatase required for the synthesis of 17-β-estradiol (E2) allows for local production of E2 in absence of functional ovaries. Understanding how aromatase activity is regulated could help alleviate the cognitive symptoms. In female rodents, genetic or pharmacological reduction of aromatase activity over extended periods of time impair memory formation, decreases spine density, and hinders long-term potentiation (LTP) in the hippocampus. Conversely, increased excitatory neurotransmission resulting in rapid N-methyl-d-aspartic acid (NMDA) receptor activation rapidly promotes neuroestrogen synthesis. This rapid modulation of aromatase activity led us to address the hypothesis that acute neuroestrogens synthesis is necessary for LTP at the Schaffer collateral-cornu ammonis 1 (CA1) synapse in absence of circulating ovarian estrogens. To test this hypothesis, we did electrophysiological recordings of field excitatory postsynaptic potential (fEPSPs) in hippocampal slices obtained from ovariectomized mice. To assess the impact of neuroestrogens synthesis on LTP, we applied the specific aromatase inhibitor, letrozole, before the induction of LTP with a theta burst stimulation protocol. We found that blocking aromatase activity prevented LTP. Interestingly, exogenous E2 application, while blocking aromatase activity, was not sufficient to recover LTP in our model. Our results indicate the critical importance of rapid, activity-dependent local neuroestrogens synthesis, independent of circulating hormones for hippocampal synaptic plasticity in female rodents.

KEYWORDS
aromatase, electrophysiology, estrogen, hippocampus, synaptic plasticity

1 | INTRODUCTION

The end of ovarian hormone production at menopause coincides with cognitive decline in women along with increased risk of dementia.[1] Although controversial, hormone therapy reduces the impact of cognitive decline during menopause in healthy subjects.[2] In rodents, exposure to 17-β-estradiol (E2) administered after ovariectomy, a rodent model of menopause, improves hippocampal-dependent memory tasks.[3,4] These benefits persist long after the end of hormone treatment[5–7] and are supported by the estrogen receptor alpha (Erα[8–11]). E2 can also support neuronal plasticity through rapid "non-genomic" means,[12,13] which involve membrane bound receptors.[14,15]

Exogenous E2 application on hippocampal slices rapidly enhances excitatory neurotransmission both presynaptically by increasing glutamate release[16,17] and postsynaptically by acting on N-methyl-d-aspartic acid (NMDA) receptors.[18,19] These synaptic effects have important consequences on a cellular correlate of learning and memory, long-term potentiation (LTP), as insertion of NMDA receptors, major contributors of calcium (Ca^{2+}) entry, are required for LTP.[20] Accordingly, when applied to hippocampal slices before LTP induction, E2 facilitates and enhances LTP.[18,21,22] It is now well accepted that tissue- and cell-specific synthesis of E2 exists outside of the ovaries, in both females and males.[23,24] Among those sources, the brain can produce E2 locally.[25–27] The hippocampus expresses the rate limiting enzyme, aromatase, which converts testosterone into E2,[28–30] allowing local production of neuroestrogen, which can be blocked by the nonsteroidal aromatase inhibitor, letrozole (LTZ,[31]).

Systemic administration of aromatase inhibitors also causes memory deficits in birds, mice and even humans, when used for breast cancer treatments.[32–36] Presumably, neuroestrogen produced in the hippocampus by aromatase activation contributes against these cognitive deficits, as chronic administration of LTZ or deletion of the aromatase gene, CYP19A1,[28] decreases spine density[37,38] and alters LTP in the hippocampus.[28,39]

Interestingly, aromatase activity is transiently modulated in under 5 min by changes in concentrations in potassium or Ca^{2+}.[40] Increased neuronal activity can stimulate neuroestrogens synthesis after glutamate activation of NMDA receptors in hippocampal preparations[25,41] and within 30 min following training for hippocampal dependent memory task.[35] This suggests that local neuroestrogens may have a stronger influence on synaptic plasticity and short-term signaling cascades over ovarian, circulating, estrogens.

In this study, we address the hypothesis that acute neuroestrogens synthesis is required for long-term potentiation of hippocampal field excitatory postsynaptic potentials (fEPSP) in absence of circulating ovarian estrogens. To test this hypothesis, we ovariectomized (OVX) young adult mice and after 10 to 18 days recorded field excitatory postsynaptic potential (fEPSPs) from the cornu ammonis 1 (CA1) pyramidal layer of hippocampal brain slices. The slices were stimulated in the Schaffer collaterals projecting from CA3 to CA1 and submitted to a theta burst stimulation (TBS) protocol to induce LTP. To assess the impact of neuroestrogens synthesis on LTP, we applied LTZ prior to the induction of LTP. We found that a 30-min inhibition of aromatase activity was enough to prevent LTP. We also investigated the impact of the application of exogenous E2 in presence or absence of aromatase activity and found concomitant application of exogenous E2 was not sufficient to recover LTP in our model.

2 | METHODS

2.1 | Animals

Sixty to 70 days old C57Bl6 female mice from Inotiv (formerly Envigo, USA) were OVX under ketamine (100 mg/kg)/xylazine (7 mg/kg) anesthesia. Buprenex (0.1 mg/kg) was administered before surgery for pain. After surgery, the animals were allowed to recover for at least 10 days and up to 18 days in individual cages to insure basal levels of estradiol in the brain.[42] The efficacy of the OVX was confirmed by measuring 1 cm of uterus weight at time of death. All animals presented atrophied uteri (4.35 ± 0.2 mg) when compared with cycling animals (18.3 ± 1. 4 mg[43]).The animals were single housed in microisolator cages with wood-based bedding (PJ Murphy Forest Products, Sani-Chips®) and had ad libitum access to water and phyto-estrogen free chow (Labdiet, 5V5R–PicoLab®) under a 12/12 h light/dark cycle (6 am/6 pm).

All animal procedures were approved by Tulane University Institutional Animal Care and Use Committee (IACUC) according to National Institutes of Health (NIH) guidelines.

2.2 | Drugs

The aromatase inhibitor LTZ (Sigma-Aldrich) was dissolved in 100% dimethyl sulfoxide (DMSO, Sigma-Aldrich) at a concentration of 1 mM and added directly into the recording bath at a final concentration of 100 nM, 0.01% DMSO. The estrogen, E2 (Sigma-Aldrich), was dissolved in 100% ethanol at a concentration of 100 µM and added directly into the recording bath at a final concentration of 10 nM in most experiments. E2 concentrations (1 and 100 nM) were also tested (Figure 2A).

2.3 | Slice preparation

Slices were prepared from mice 10 to 18 days after OVX, which allowed circulating E2 levels to drop significantly.[44,45] The mice were anesthetized with isoflurane and decapitated. Brains were quickly removed and immersed in oxygenated (95% O_2 and 5% CO_2), ice-cold N-methyl-D-glucamine (NMDG)-based slicing solution (in millimoles, 110 NMDG, 3 KCl, 1.1 NaH_2PO_4, 25 $NaHCO_3$, 25 glucose, 10 ascorbic acid, 3 pyruvic acid, 10 $MgSO_4$, 0.5 $CaCl_2$, pH to 7.3–7.4 with HCl).[46] Following the procedure described in Bischofberger et al.,[47] 400 µM horizontal brain sections preserving the Schaffer collaterals in the hippocampus were obtained with a Vibratome Series 3000 Plus Tissue Sectioning System. The freshly collected brain slices were incubated

at 37°C for 15 min in NMDG, then transferred and incubated in oxygenated artificial cerebrospinal fluid (aCSF, in mM, NaCl 124, KCl 2.5, NaH_2PO_4 1.06, $NaHCO_3$ 25, Glucose 14.5, $MgCl_2$ 2, $CaCl_2$ 2) at room temperature until use.

2.4 | Electrophysiology recordings

Field recordings were acquired using a MultiClamp 700a amplifier, Digidata 1322A digitizer, and a personal computer running Clampex 10.3 software (Molecular Device). Data were sampled at 10 kHz.

Hippocampal slices were placed in a chamber perfused with oxygenated aCSF at 31°C. A tungsten bipolar electrode was placed in CA2/CA3 region to stimulate the Schaffer collaterals. A glass pipette (1–3 mΩ) filled with aCSF was placed in the *stratum radiatum* of CA1 to record fEPSPs. fEPSPs were evoked every 10 s to monitor their evolution over time. The stimulus intensity was set to a range of 30 to 50% of the maximal response, defined from an input–output curve (0–10 mA stimulation intensity, Figure 1). After at least 20 min of stable recording, either drugs or a long-term potentiation (LTP) protocol was applied. The drugs were applied in the circulating aCSF for at least 30 min until the fEPSPs were stable for 10 min. These 10 min were used as a baseline for post-TBS LTP. The LTP protocol consisted of TBS design as four bursts at 100 Hz every 200 ms repeated four times every 20 s. After the TBS, fEPSPs were monitored every 10 s for 60 min.

2.5 | Paired-pulse facilitation

Paired-pulse facilitation was assessed by applying two consecutive pulses at the intensity defined by the input–output curve as described above. The time intervals used between the two pulses were 25, 50, 75, and 100 ms. The ratio was calculated by dividing the second peak amplitude by the first peak amplitude (PPR = Peak Amp2/Peak Amp 1).

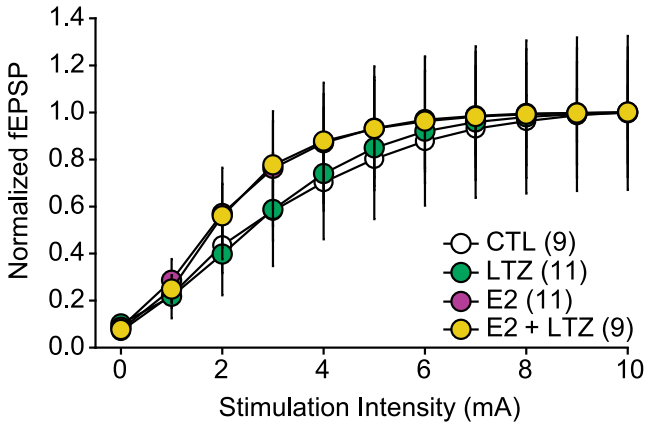

FIGURE 1 The input–output curves are not significantly different between control (CTL, $n = 9$), letrozole (LTZ, $n = 11$), 17-β-estradiol (E2, $n = 11$) and E2 + LTZ ($n = 9$) groups. Interaction: $F(27,324) = 0.274$, $p = .897$; Time: $F(9,324) = 45.823$, $p < .001$; Group: $F(3,36) = 0.41$, $p > .05$. Field excitatory postsynaptic potential (fEPSP) (*y*-axis) are normalized to the maximum fEPSP.

2.6 | Statistics

Data are reported as mean ± SEM. Statistics were done using IBM SPSS statistics software (SPSS inc, Windows Version 28.0.0.0, Chicago). Data were analyzed by Student *t*-tests, one-way, and two-way repeated measures ANOVA with Greenhouse–Geisser correction, Tukey, or pairwise comparisons with Sidak adjustment post hoc tests as described in the statistical Table 1.

3 | RESULTS

3.1 | Field EPSP stimulation intensity setting

Input–output curves measuring the relationship of stimulus intensity and fEPSP slope were determined at baseline before TBS and drug application (Figure 1). No significant differences in the input–output curves of all four groups (Vehicle, LTZ, E2, E2 + LTZ) were observed ($F(3,37) = 0.42$, $p = .989$). To assess LTP, the stimulation intensities of the fEPSP were set within a range of 30%–50% of the maximum intensity observed.

3.2 | Effect of drugs on baseline fEPSP

Baseline field EPSPs were recorded for at least 20 min to establish a stable baseline before drugs were applied in the bath (Figure 2A,B). After the addition of the drugs, fEPSP were monitored until a new 10-min stable baseline was established usually 20–30 min after the drug application.

As the literature reports effects of E2 on baseline synaptic transmission at concentrations ranging between 1 and 100 nM,[11,16,39,48] we tested the effect of 3 different concentrations of E2 (1, 10, and 100 nM) on fEPSP baseline (Figure 2A). E2 application (1 and 10 nM) increased fEPSP slope to 109 ± 26% ($t(7) = 1.771$, $p = .12$) and 121% ± 26% ($t(10) = 3.735$, $p = .004$) of baseline, respectively. The 100 nM concentration increased fEPSP slope to 221% ± 70% of baseline measures (Figure 2A). Application of 10 nM of E2 significantly increased the fEPSP slope from −0.15 ± 0.03 to −0.19 ± 0.04 mV/ms ($t(10) = 3.7335$, $p = 0.004$, Figure 2A,B). To keep enough margin for LTP development, while having confirmation that E2 was effective, we chose to use 10 nM.

Application of a commonly used dose of LTZ (100 nM,[37,39,48–52]) also slightly but significantly increased the baseline fEPSP slope with the slope changing from −0.12 ± 0.03 mV/ms at baseline to −0.13 ± 0.03 mV/ms after LTZ, $t(10) = 2.887$, $p = 0.016$ (Figure 2B). While the combined application of E2 (10 nM) and LTZ (100 nM) did not

TABLE 1 Statistical analysis table.

	Title	Distribution	Test	Results	*p* value	Power	
Figure 1	Input–Output curves	Mauchly's test of sphericity failed ($p < .001$)	2-way ANOVA Time Group Interaction	Greenhouse–Geisser $F(9,324) = 45.82$ $F(3,36) = 0.41$ $F(27,324) = 0.27$	.001 .989 .897	1 0.056 0.106	NA (Not Applicable)

Figure	Title	Distribution Shapiro–Wilk	Test	Results	*p* value	Power	Post hoc	Groups	95% confidence interval
Figure 2A	E2 (1 nM) on fEPSP	Normality passed, $p = .16$	Paired sample *t*-test (two-sided)	$t(7) = 1.77$	.12	2-tailed, 95% = 0.40	NA	Baseline versus drug	−0.15 1.30
Figure 2B	E2 (100 nM) on fEPSP	Normality passed, $p = .33$	Paired sample *t*-test (two-sided)	$t(3) = 1.51$	.22	2-tailed, 95% = 0.19	NA	Baseline versus drug	−0.35 0.97
Figure 2B	LTZ (100 nM) on fEPSP	Normality passed, $p = .48$	Paired sample *t*-test (two-sided)	$t(10) = 2.89$	.02	2-tailed, 95% = 0.74	NA	Baseline versus drug	0.003 0.024
Figure 2A,B	E2 (10 nM) on fEPSP	Normality passed, $p = .47$	Paired sample *t*-test (two-sided)	$t(10) = 3.73$	.004	2-tailed, 95% = 0.9	NA	Baseline versus drug	0.01 0.05
Figure 2B	E2 + LTZ on fEPSP	Normality passed, $p = .30$	Paired sample *t*-test (two-sided)	$t(8) = 1.84$	.10	2-tailed, 95% = 0.37	NA	Baseline versus drug	−0.008 0.075

Figure	Title	Distribution	Test	Results	*p* value	Power	Post hoc
Figure 3	LTZ paired-pulse ratio	Mauchly's test of sphericity failed ($p < .018$)	2-way ANOVA Time Group Interaction	Greenhouse–Geisser $F(3,18) = 33.0$ $F(1,6) = 1.03$ $F(3,18) = 1.26$	.001 .35 .32	.99 .14 .18	NA

Figure	Title	Distribution	Test	Results	*p* value	Power	Post hoc
Figure 4E	fEPSP LTP time course in 10-min bins	Mauchly's Test of Sphericity Failed ($p < .000$)	2-way ANOVA Time Group Interaction	Greenhouse–Geisser $F(6,216) = 15.93$ $F(3,36) = 5.62$ $F(18,216) = 2.784$	.001 .003 .004	1 0.92 0.96	Pairwise with Sidak adjustment

Figure 4E continued: Pairwise comparisons with Sidak adjustment for multiple comparisons:

Time	Group	Versus	Lower	Upper	*p* value
Time 1 (Baseline: −10 to 0′)	Control	LTZ	0.004	0.015	.025
		E2	0.002	0.013	.129
		E2 + LTZ	0.002	0.014	.083
	LTZ	Control	−0.015	−0.004	.025
		E2	−0.007	0.003	.98
		E2 + LTZ	−0.007	0.004	1
	E2	Control	−0.013	−0.002	.129
		LTZ	−0.003	0.007	.98
		E2 + LTZ	−0.006	0.006	1
	E2 + LTZ	Control	−0.014	−0.002	.083
		LTZt	−0.004	0.007	1
		E2	−0.006	0.006	1
Time 2 (0′ to 10′)	Control	LTZ	−0.04	0.305	.548
		E2	−0.011	0.334	.333
		E2 + LTZ	−0.107	0.254	.961

TABLE 1 (Continued)

Figure 4E continued: Pairwise comparisons with Sidak adjustment for multiple comparisons:

Time	Group	Versus	Lower	Upper	*p* value
	LTZ	Control	−0.305	0.04	.548
		E2	−0.134	0.193	1
		E2 + LTZ	−0.231	0.114	.98
	E2	Control	−0.334	0.011	.333
		LTZ	−0.193	0.134	1
		E2 + LTZ	−0.26	0.085	.888
	E2 + LTZ	Control	−0.254	0.107	.961
		LTZ	−0.114	0.231	.98
		E2	−0.085	0.26	.888
Time 3 (10′ to 20′)	Control	LTZ	0.033	0.458	.139
		E2	−0.083	0.342	.776
		E2 + LTZ	−0.05	0.396	.545
	LTZ	Control	−0.458	−0.033	.139
		E2	−0.318	0.085	.828
		E2 + LTZ	−0.285	0.14	.983
	E2	Control	−0.342	0.083	.776
		LTZet	−0.085	0.318	.828
		E2 + LTZ	−0.169	0.257	.999
	E2 + LTZ	Control	−0.396	0.05	.545
		LTZ	−0.14	0.285	.983
		E2	−0.257	0.169	.999
Time 4 (20′ to 30′)	Control	LTZ	0.13	0.622	.022
		E2	−0.049	0.443	.509
		E2 + LTZ	0.086	0.603	.058
	Lt	Control	−0.622	−0.13	.022
		E2	−0.413	0.054	.565
		E2 + LTZ	−0.278	0.215	1
	E2	Control	−0.443	0.049	.509
		LTZ	−0.054	0.413	.565
		E2 + LTZ	−0.098	0.394	.79
	E2 + LT	Control	−0.603	−0.086	.058
		LTZ	−0.215	0.278	1
		E2	−0.394	0.098	.79
Time 5 (30′ to 40′)	Control	LTZ	0.15	0.598	.01
		E2	−0.049	0.399	.552
		E2 + LTZ	0.131	0.6	.019
	LTZ	Control	−0.598	−0.15	.01
		E2	−0.412	0.013	.323
		E2 + LT	−0.232	0.216	1
	E2	Control	−0.399	0.049	.552
		LTZ	−0.013	0.412	.323
		E2 + LTZ	−0.033	0.415	.433
	E2 + Let	Control	−0.6	−0.131	.019
		LTZ	−0.216	0.232	1
		E2	−0.415	0.033	.433

(Continues)

TABLE 1 (Continued)

Figure 4E continued: Pairwise comparisons with Sidak adjustment for multiple comparisons:

Time	Group	Versus	Lower	Upper	*p* value
Time 6 (40′ to 50′)	Control	LTZ	0.226	0.625	<.001
		E2	0.047	0.446	.099
		E2 + LTZ	0.21	0.63	.001
	LTZ	Control	−0.625	−0.226	<.001
		E2	−0.369	0.01	.322
		E2 + LTZ	−0.205	0.194	1
	E2	Control	−0.446	−0.047	.099
		LTZ	−0.01	0.369	.322
		E2 + LTZ	−0.026	0.373	.409
	E2 + LTZ	Control	−0.63	−0.21	.001
		LTZ	−0.194	0.205	1
		E2	−0.373	0.026	.409
Time 7 (50′ to 60′)	Control	LTZ	0.189	0.633	.004
		E2	0.007	0.451	.234
		E2 + LTZ	0.174	0.639	.006
	LTZ	Control	−0.633	−0.189	.004
		E2	−0.392	0.028	.419
		E2 + LTZ	−0.226	0.217	1
	E2	Control	−0.451	−0.007	.234
		LTZ	−0.028	0.392	.419
		E2 + LTZ	−0.044	0.399	.504
	E2 + LT	Control	−0.639	−0.174	.006
		LT	−0.217	0.226	1
		E2	−0.399	0.044	.504

Figure	Title	Distribution	Test	Results	*p* value	Power	Post hoc
Figure 4F	Fiber volley LTP time course in 10-min bin	Mauchly's test of sphericity failed ($p < .000$)	2-way ANOVA Time Group Interaction	Greenhouse–Geisser $F(6,216) = 1.79$ $F(3,36) = 1.53$ $F(18,216) = 0.96$	.10 .22 .51	0.38 0.37 0.38	NA

Figure	Title	Distribution	Test	Results	*p* value	Power	Post hoc
Figure 4G	fEPSP change Bar graph last 10 min	Normality and equality of variance passed Normality, $p = .124$ Eq of variance: $p = .183$	One way ANOVA	$F(3,39) = 6.53$	.001	0.92	Tukey HSD

Figure 4G continued

Post hoc	Groups	*p* value	95% interval of confidence		
Tukey HSD	Group	Vs	Lower	Upper	*p* value
	Control	Let	10.1414	56.4994	.002
		Estradiol	−9.6459	36.7121	.407
		E2 + LTZ	7.0786	55.6992	.007
	LTZ	Control	−56.4994	−10.1414	.002
		Estradiol	−41.7768	2.2023	.091
		E2 + LTZ	−25.1105	21.2475	.996

TABLE 1 (Continued)

Figure 4G continued							
Post hoc	**Groups**	***p* value**	**95% interval of confidence**				
Tukey HSD	**Group**	**Vs**	**Lower**	**Upper**			***p* value**
	Estradiol	Control	−36.7121	9.6459			.407
		LTZ	−2.2023	41.7768			.091
		E2 + LTZ	−5.3232	41.0348			.181
	E2 + LTZ	Control	−55.6992	−7.0786			.007
		LTZ	−21.2475	25.1105			.996
		Estradiol	−41.0348	5.323			.181
Figure	**Title**	**Distribution**	**Test**	**Results**	***p* value**	**Power**	**Post hoc**
Figure 4H	Fiber volley change bar graph last 10 min	Normality and equality of variance passed Normality, $p = .74$ Eq. of variance, $p = .92$	One-way ANOVA	$F(3,39) = 0.08$	.97	0.049	NA

Abbreviations: E2, 17-β-estradiol; fEPSP, field excitatory postsynaptic potential; LTZ, letrozole; LTP, long-term potentiation; NA, not applicable.

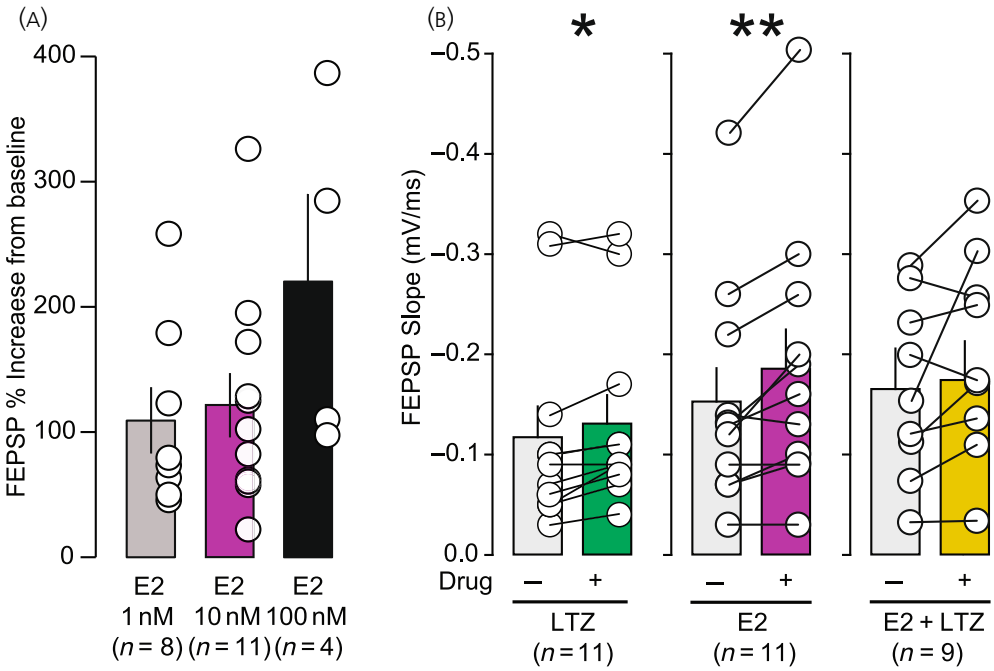

FIGURE 2 (A) Effect of 1, 10, 100 nM of 17-β-estradiol (E2) on basal field excitatory postsynaptic potential (fEPSP). Values are normalized to baseline. E2 1 nM: $T(7) = 1.771$, $p = .120$, $n = 11$; E2 10 nM: $T(10) = 3.735$, $p = .004$, $n = 11$; E2 100 nM: $T(3) = 1.509$, $p = .120$, $n = 4$. (B) Effect of letrozole (LTZ) (100 nM, $n = 11$), E2 (10 nM, 11), and LTZ + E2 (100/10 nM, $n = 9$) on basal fEPSP slope. Both LTZ ($p < .05$) and E2 ($p < .01$) significantly increased fEPSP slope. LTZ 100 nM: $T(10) = 2.887$, $p = .016$; E2 10 nM: $T(10) = 3.735$, $p = .004$; LTZ + E2 100/10 nM: $T(8) = 1.840$, $p = .103$.*$p < .05$, **$p < .01$, ***$p < .001$.

significantly change the slope (baseline: −0.16 ± 0.03 mV/ms, E2 + LTZ: −0.20 ± 0.03 mV/ms, $t(8) = 1.084$, $p = 0.103$, Figure 2B).

3.3 | Paired-pulse ratio with LTZ

As previous studies showed that E2 can enhance the glutamate release probability of the Schaffer collaterals in the hippocampus,[16,17] and LTZ affects the synthesis of neuroestrogens in the hippocampus, we determined LTZ's effect on release probability in our preparation. To study the release probability, we used the paired-pulse ratio (PPR), which is the ratio between two evoked postsynaptic events given within a short period of time (Figure 3).[53–55] LTZ did not significantly affect the PPR, at any of the inter-pulse intervals tested (Figure 3, effect of treatment: $F(1,31) = 1.211$, $p = 0.35$). These data indicate that blocking neuroestrogen synthesis with LTZ did not significantly affect the probability of glutamate release from presynaptic terminals.

3.4 | Long-term potentiation

TBS was applied to induce LTP after at least 10 min of stable baseline fEPSPs. In the control group, TBS induced an increase in the fEPSP

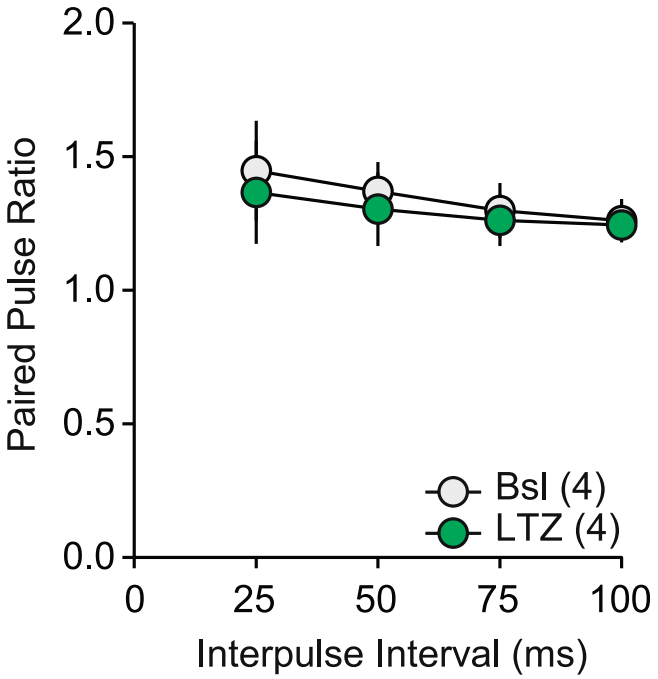

FIGURE 3 Thirty minutes application of letrozole (LTZ) did not significantly change the paired-pulse ratio of Schaffer collateral to CA1 synapse in the hippocampus. Interaction: $F(3,18) = 1.261$, $p = .317$; Time: $F(3,18) = 33.025$, $p < .001$; Group: $F(1,6) = 1.028$, $p = .350$.

slope to 148 ± 8% (Figure 4A,E,G) compared with baseline value after 50–60 min. The slope of the fiber volley, which reflects the presynaptic activity, remained constant (104 ± 6%), during the same time lapse (Figure 4A,F,H). When the TBS protocol was given in presence of LTZ, fEPSP slope increased to only 112 ± 6% from baseline (Figure 4B,E,G), while the fiber volley also remained constant (105 ± 5%, Figure 4B,F,H). This result shows that LTZ blocked TBS-induced potentiation.

When the TBS was applied in the presence of E2 (10 nM), the fEPSP slope increased similarly to the control conditions to 131 ± 6% (Figure 4C,E,G) compared with pre-TBS baseline and the volley fiber was not affected (102 ± 5%, Figure 4C,F,H).

As blocking the synthesis of neuroestrogen with LTZ prevented the development of LTP, we assessed the ability of exogenous E2 to rescue it by adding E2 (10 nM) during LTZ application before inducing LTP. In these conditions, LTP was reduced and the fEPSP slope increased by 113 ± 4% from baseline (Figure 4D,E,G). Again, the fiber volley slope remained constant (104 ± 6%, Figure 4D,F,H).

When compared, the LTP levels revealed a significant difference ($F(3,37) = 6.374$, $p = .001$) with the post hoc analysis indicating that both LTZ ($p = .002$) and E2 + LTZ ($p = .008$) groups were different from the control group (Figure 4E,G). The E2 group was not significantly different from the control group ($p = .403$), the LTZ group ($p = .09$), nor the E2 + LTZ group ($p = .224$). The LTZ group and the E2 + LTZ group also were not different ($p = .976$). This result shows that while LTZ blocked TBS-induced potentiation, exogenous E2 was not able to rescue it.

4 | DISCUSSION

In this study, we investigated the role of local estrogen synthesis during the induction of LTP in the CA1 region of the hippocampus in slices from OVX female mice. We show that aromatase activity, and rapid neuroestrogen synthesis within the hippocampus, are required during TBS for the induction of LTP in absence of circulating ovarian hormones and cannot be recovered with bath application of exogenous E2 (10 nM).

Consistent with previous studies that have showed that either chronic inhibition of neuroestrogen synthesis by pharmacological inhibition[39] or genetic knockout[28] of aromatase impair LTP and memory formation in female mice,[11] our results extend these studies showing that an acute inhibition of aromatase also impairs induction of LTP independent of any long-term, transcriptional alterations in OVX females.

A crucial question of our study is related to the role of neuroestrogen versus circulating estrogens on hippocampal synaptic plasticity. Our results point to a critical and specific role of locally produced neuroestrogens in LTP induction as exogenous application of E2 did not rescue the LTZ-induced inhibition of LTP. Consistent with our results are a series of studies that show the importance of locally synthesized and not ovarian or exogenous estrogens in hippocampal synaptic plasticity and dendritic spine dynamics.[38,56,57] Chemical or genetic inactivation of aromatase lead to a reduction in spine numbers in the hippocampus.[28,58] Echoing our results, in vitro application of exogenous low, physiological concentrations of E2 (0.1–10 nM) was not able to rescue the LTZ-mediated decrease in synaptophysin expression[37] or the upregulation of the immediate early gene Arc/Arg3.1,[59] indicating that exogenous E2 application alone is not always sufficient to compensate for loss of aromatase activity and neuroestrogen synthesis.

But our observation is also at odds with other studies that showed exogenous E2 application rescued LTZ inhibition of LTP. For example, acute administration of 0.2 nM E2 was able to rescue HFS induced LTP in hippocampus slices from male mice.[50] In females, both 1 and 100 nM E2 were able to recover LTP in slices of OVX mice either knocked-down for aromatase[28] or chronically treated with LTZ,[39] as well as in cycling mice chronically treated with the aromatase inhibitor, formestane.[11]

Multiple reasons could explain this discrepancy of the role of exogenous E2 in recovery aromatase-dependent LTP, including sex differences[60] or ovarian hormone status. Ovariectomy and even estrous cycle could also influence E2 sensitivity, as spine density changes with estrous stage.[61,62] In addition, compensatory mechanisms in both genetic and chronic inhibition of aromatase, involving translational or transcriptional modifications may have taken place altering the systems sensitivity to E2, which may not be present under rapid conditions of acute applications in brain slices. One could also argue that application of E2 simply had no effect in our hands. However, we observed an increase in the amplitude of basal fEPSP slope within minutes after E2 application, consistent with previous studies.[16,21,63,64] This acute increase in basal excitatory transmission

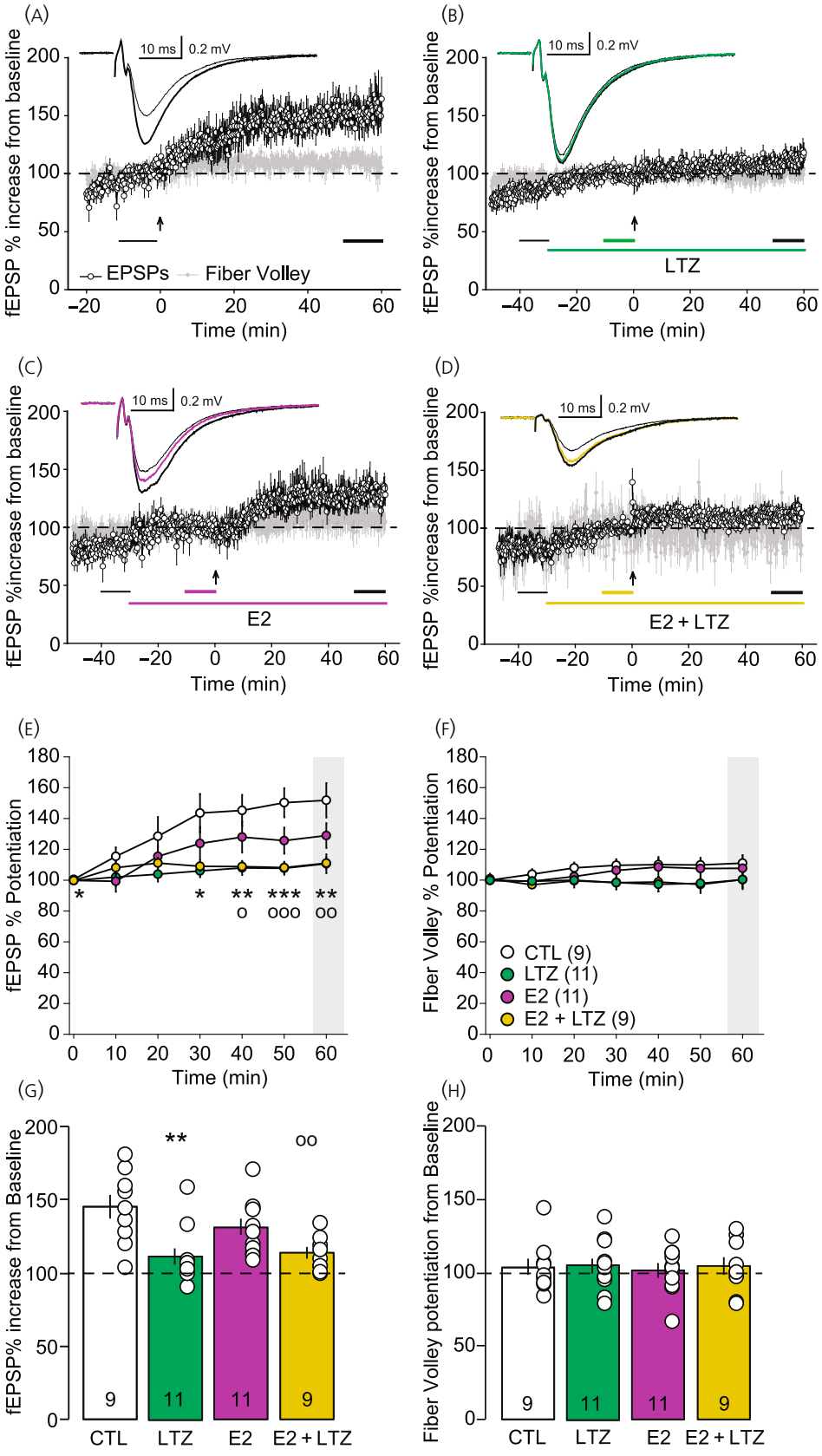

FIGURE 4 Legend on next page.

produced by E2 is driven by at least two mechanisms, including a direct stimulation of excitatory neurotransmission through ERβ,[17] or a more complex pathway relying on ERα and involving mGluR1 and endocannabinoids to suppress inhibitory interneuron firing.[65] In either framework, the studies report that only a subset of hippocampal neurons responds to E2 acting on the release probability of a group of synapses that have an overall effect on the local network.[66] Also the estrogen receptors, Erα, Erβ, and GPER1 distribution and sensitivity for E2 modulate the network activity in as levels of hormones fluctuate.[61] Given the complexity of the hippocampal microcircuits, the impact of E2, whether exogenous or local, and on inhibitory neurotransmission makes the overall output difficult to predict.[67]

Surprisingly, in our experiments, acute application of LTZ, like E2, caused an increase in the baseline fEPSP slope. This increase was small but significant and there was no effect on presynaptic glutamate release, as paired-pulse facilitation was unchanged by LTZ.

When both exogenous E2 and LTZ were applied together, the combination occluded the increase in fEPSP slope, suggesting that exogenous E2 and neuroestrogen may ultimately act through similar mechanisms to affect baseline activity. This could be due to a shift in the neurosteroid synthesis pathway, as LTZ prevents the transformation of testosterone to E2. With this blockade of aromatase, testosterone may instead be converted into dihydrotestosterone (DHT) by the 5α-reductase type 2.[68,69] Interestingly, previous studies have shown that DHT synthesis is necessary for long-term depression in response to 1 Hz stimuli in male rats.[50,51,70] In our case of the LTZ-induced increase in basal transmission, DHT may counteract the potentiating effect of E2 to prevent the E2-induced increase in basal transmission. Our study here does not address the role of DHT in basal transmission or activity-dependent plasticity, but future studies need to focus on whether other neurosteroids affect basal transmission or activity-dependent plasticity as well as any differences across sexes.

In summary, our current study adds to a growing literature that supports the hypothesis that locally produced estrogens have a greater impact on hippocampal physiology than circulating estrogens.[60,71–73] Given the impact of the loss of ovarian hormones at menopause on cognitive functions, understanding the mechanisms by which the brain can synthetize neuroestrogen is becoming more and more relevant in our aging society. Our study comes in support of other studies showing the requirement of local neuroestrogen synthesis for hippocampal memory formation adding the observation of the reliance of the LTP induction on neuroestrogens when ovarian hormones are removed. The intrinsic relationship and timing between the machineries engaged by both the LTP process and estrogens still need better understanding to eventually improve treatment alleviating menopausal effects on aging women cognition.

AUTHOR CONTRIBUTIONS

Matthieu J. Maroteaux: Conceptualization; data curation; formal analysis; investigation; methodology; project administration; software; visualization; writing – original draft. **Claire T. Noccioli:** Investigation. **Jill M. Daniel:** Conceptualization; funding acquisition; project administration; resources; supervision; writing – original draft. **Laura A. Schrader:** Conceptualization; data curation; formal analysis; methodology; project administration; supervision; writing – original draft.

ACKNOWLEDGEMENTS

This work was supported by grant RF1AG041374 of the National Institute on Aging to Jill M. Daniel.

CONFLICT OF INTEREST STATEMENT

The authors declare no conflicts of interest.

PEER REVIEW

The peer review history for this article is available at https://www.webofscience.com/api/gateway/wos/peer-review/10.1111/jne.13450.

FIGURE 4 Time course and analysis of long-term potentiation (LTP) of Schaffer collateral to CA1 synapse in the hippocampus. (A) Time course of slope of field excitatory postsynaptic potential (fEPSP) (open circles) and fiber volley (gray circles) in control condition (CTL, $n = 9$), in absence of any treatment sampled every 10 s; insert: Average traces 10 min before (thin gray trace) and 50 min after theta burst stimulation (TBS, black trace). (B) Time course of slope of fEPSP (open circles) and fiber volley (gray circles) in presence of letrozole (LTZ) (100 nM, $n = 11$) sampled every 10 s; insert: Average traces 10 min before LTZ application (thin black trace), 20 min after LTZ application (green trace) and 50 min after TBS (thick black trace). (C) Time course of slope of fEPSP (open circles) and fiber volley (gray circles) in presence of 17-β-estradiol (E2) (10 nM, $n = 11$) sampled every 10 s; insert: Average traces 10 min before E2 application (thin black trace), 20 min after LTZ application (purple trace) and 50 min after TBS (thick black trace). (D) Time course of fEPSP (open circles) and fiber volley (gray circles) in presence of E2 (1 nM) and LTZ (100 nM) sampled every 10 s ($n = 9$); insert: Average traces 10 min before E2 application (thin black trace), 20 min after drug application (yellow trace) and 50 min after TBS (thick black trace). In (A)–(D), the long-colored line indicates when the drugs are applied; the arrow indicates the time at which the TBS was applied; the two or three short bottom lines indicate the periods over which the traces represented in the insert were averaged as well as the averaged values used in (G) and (H). (E) Development of the fEPSP after the LTP induction represented in 10-min bin. Interaction: $F(18,216) = 2.784$, $p < .004$; Time: $F(6,216) = 15.932$, $p < .001$; Group: $F(3,36) = 5.623$, $p = .003$. (F) Development of the fiber volley after the LTP induction represented in 10 min bin. Interaction: $F(18,216) = .955$, $p = .514$; Time: $F(6,216) = 1.788$, $p = .103$; Group: $F(3,36) = 1.529$, $p = .224$. In (E) and (F), the time 0 min corresponds to the baseline before TBS to which the values have been normalized. (G) Bar graph representation of the last 10 min of fEPSP recordings relative to baseline (indicated by the short black line in A). $F(3,39) = 6.527$, $F(3,39) = 6.527$. (H) Bar graph representation of the last 10 min of fiber volley recordings relative to baseline (indicated by the short black line in C). $F(3,39) = 0.078$, $p = .971$. Post hoc statistics for (E) and (G): $^{*}p < .05$, $^{**}p < .01$, $^{***}p < .001$ CTL versus LTZ and $\circ p < .05$, $\circ\circ p < .01$, $\circ\circ\circ p < .001$, CTL versus E2 + LTZ.

DATA AVAILABILITY STATEMENT

The data that supports the findings of this study are available in the supplementary material of this article.

ORCID

Matthieu J. Maroteaux https://orcid.org/0000-0003-2694-0773

REFERENCES

1. Scheyer O, Rahman A, Hristov H, et al. Female sex and Alzheimer's risk: the menopause connection. *J Prev Alzheimers Dis*. 2018;5:225-230.
2. Pines A. Alzheimer's disease, menopause and the impact of the estrogenic environment. *Climacteric*. 2016;19:430-432.
3. Daniel JM, Hulst JL, Berbling JL. Estradiol replacement enhances working memory in middle-aged rats when initiated immediately after Ovariectomy but not after a long-term period of ovarian hormone deprivation. *Endocrinology*. 2006;147:607-614.
4. Frick KM. Estrogens and age-related memory decline in rodents: what have we learned and where do we go from here? *Horm Behav*. 2009;55:2-23.
5. Luine VN. Estradiol and cognitive function: past, present and future. *Horm Behav*. 2014;66:602-618.
6. Smith CC, Vedder LC, Nelson AR, Bredemann TM, McMahon LL. Duration of estrogen deprivation, not chronological age, prevents estrogen's ability to enhance hippocampal synaptic physiology. *Proc Natl Acad Sci U S A*. 2010;107:19543-19548.
7. Vedder LC, Bredemann TM, McMahon LL. Estradiol replacement extends the window of opportunity for hippocampal function. *Neurobiol Aging*. 2014;35:2183-2192.
8. Foster TC, Rani A, Kumar A, Cui L, Semple-Rowland SL. Viral vector–mediated delivery of estrogen receptor-α to the hippocampus improves spatial learning in estrogen receptor-α knockout mice. *Mol Ther*. 2008;16:1587-1593.
9. Pollard KJ, Wartman HD, Daniel JM. Previous estradiol treatment in ovariectomized mice provides lasting enhancement of memory and brain estrogen receptor activity. *Horm Behav*. 2018;102:76-84.
10. Rodgers SP, Bohacek J, Daniel JM. Transient estradiol exposure during middle age in ovariectomized rats exerts lasting effects on cognitive function and the hippocampus. *Endocrinology*. 2010;151:1194-1203.
11. Wang W, Le AA, Hou B, et al. Memory-related synaptic plasticity is sexually dimorphic in rodent hippocampus. *J Neurosci*. 2018;38:7935-7951.
12. Kalita K, Szymczak S, Kaczmarek L. Non-nuclear estrogen receptor beta and alpha in the hippocampus of male and female rats. *Hippocampus*. 2005;15:404-412.
13. Vasudevan N, Pfaff DW. Non-genomic actions of estrogens and their interaction with genomic actions in the brain. *Front Neuroendocrinol*. 2008;29:238-257.
14. Fuentes N, Silveyra P. Estrogen receptor signaling mechanisms. *Adv Protein Chem Struct Biol*. 2019;116:135-170.
15. Hojo Y, Murakami G, Mukai H, et al. Estrogen synthesis in the brain—role in synaptic plasticity and memory. *Mol Cell Endocrinol*. 2008;290:31-43.
16. Oberlander JG, Woolley CS. 17β-estradiol acutely potentiates glutamatergic synaptic transmission in the hippocampus through distinct mechanisms in males and females. *J Neurosci*. 2017;37:12314-12327.
17. Smejkalova T, Woolley CS. Estradiol acutely potentiates hippocampal excitatory synaptic transmission through a presynaptic mechanism. *J Neurosci*. 2010;30:16137-16148.
18. Smith CC, Vedder LC, McMahon LL. Estradiol and the relationship between dendritic spines, NR2B containing NMDA receptors, and the magnitude of long-term potentiation at hippocampal CA3–CA1 synapses. *Psychoneuroendocrinology*. 2009;34:S130-S142.
19. Weiland NG. Estradiol selectively regulates agonist binding sites on the N-methyl-D-aspartate receptor complex in the CA1 region of the hippocampus. *Endocrinology*. 1992;131:662-668.
20. Lüscher C, Malenka RC. NMDA receptor-dependent long-term potentiation and long-term depression (LTP/LTD). *Cold Spring Harb Perspect Biol*. 2012;4:a005710.
21. Foy MR, Baudry M, Akopian GK, Thompson RF. Regulation of hippocampal synaptic plasticity by estrogen and progesterone. *Vitam Horm*. 2010;82:219-239.
22. Smith CC, McMahon LL. Estrogen-induced increase in the magnitude of long-term potentiation occurs only when the ratio of NMDA transmission to AMPA transmission is increased. *J Neurosci*. 2005;25:7780-7791.
23. Barakat R, Oakley O, Kim H, Jin J, Ko CJ. Extra-gonadal sites of estrogen biosynthesis and function. *BMB Rep*. 2016;49:488-496.
24. Cui J, Shen Y, Li R. Estrogen synthesis and signaling pathways during aging: from periphery to brain. *Trends Mol Med*. 2013;19:197-209.
25. Hojo Y, Higo S, Ishii H, et al. Comparison between hippocampus-synthesized and circulation-derived sex steroids in the hippocampus. *Endocrinology*. 2009;150:5106-5112.
26. Stanić D, Dubois S, Chua HK, et al. Characterization of aromatase expression in the adult male and female mouse brain. I. Coexistence with oestrogen receptors α and β, and androgen receptors. *PLoS One*. 2014;9:e90451.
27. Toda K, Okada Y, Zubair M, Morohashi K, Saibara T, Okada T. Aromatase-knockout mouse carrying an estrogen-inducible enhanced green fluorescent protein gene facilitates detection of estrogen actions in vivo. *Endocrinology*. 2004;145:1880-1888.
28. Lu Y, Sareddy GR, Wang J, et al. Neuron-derived estrogen regulates synaptic plasticity and memory. *J Neurosci*. 2019;39:2792-2809.
29. Prange-Kiel J, Rune GM. Direct and indirect effects of estrogen on rat hippocampus. *Neuroscience*. 2006;138:765-772.
30. Simpson ER, Mahendroo MS, Means GD, et al. Aromatase cytochrome P450, the enzyme responsible for estrogen biosynthesis. *Endocr Rev*. 1994;15:342-355.
31. Prange-Kiel J, Wehrenberg U, Jarry H, Rune GM. Para/autocrine regulation of estrogen receptors in hippocampal neurons. *Hippocampus*. 2003;13:226-234.
32. Bender CM, Sereika SM, Brufsky AM, et al. Memory impairments with adjuvant anastrozole versus tamoxifen in women with early-stage breast cancer. *Menopause*. 2007;14:995-998.
33. Oberlander JG, Schlinger BA, Clayton NS, Saldanha CJ. Neural aromatization accelerates the acquisition of spatial memory via an influence on the songbird hippocampus. *Horm Behav*. 2004;45:250-258.
34. Phillips KA, Ribi K, Fisher R. Do aromatase inhibitors have adverse effects on cognitive function? *Breast Cancer Res*. 2011;13:203.
35. Tuscher JJ, Szinte JS, Starrett JR, et al. Inhibition of local estrogen synthesis in the hippocampus impairs hippocampal memory consolidation in ovariectomized female mice. *Horm Behav*. 2016;83:60-67.
36. Underwood EA, Rochon PA, Moineddin R, et al. Cognitive sequelae of endocrine therapy in women treated for breast cancer: a meta-analysis. *Breast Cancer Res Treat*. 2018;168:299-310.
37. Kretz O. Hippocampal synapses depend on hippocampal estrogen synthesis. *J Neurosci*. 2004;24:5913-5921.
38. Zhou L, Fester L, von Blittersdorff B, et al. Aromatase inhibitors induce spine synapse loss in the hippocampus of Ovariectomized mice. *Endocrinology*. 2010;151:1153-1160.
39. Vierk R, Brandt N, Rune GM. Hippocampal estradiol synthesis and its significance for hippocampal synaptic stability in male and female animals. *Neuroscience*. 2014;274:24-32.
40. Charlier TD, Cornil CA, Patte-Mensah C, Meyer L, Mensah-Nyagan AG, Balthazart J. Local modulation of steroid action: rapid control of enzymatic activity. *Front Neurosci*. 2015;9:83.

41. Kimoto T, Tsurugizawa T, Ohta Y, et al. Neurosteroid synthesis by cytochrome p450-containing systems localized in the rat brain hippocampal neurons: N-methyl-D-aspartate and calcium-dependent synthesis. *Endocrinology*. 2001;142:3578-3589.
42. Woolley CS, McEwen BS. Roles of estradiol and progesterone in regulation of hippocampal dendritic spine density during the estrous cycle in the rat. *J Comp Neurol*. 1993;336:293-306.
43. DeLarge AF, Stanley MJ, Daniel JM. Female mice lacking membrane estrogen receptor alpha display impairments in spatial memory. *Horm Behav*. 2024;164:105597.
44. Kato A, Hojo Y, Higo S, et al. Female hippocampal estrogens have a significant correlation with cyclic fluctuation of hippocampal spines. *Front Neural Circuits*. 2013;7:149.
45. Moiety FM, Salem HA, Mehanna RA, Abdel-Ghany BS. Comparative study on induction and effects of surgical menopause in a female rat model: a prospective case control study. *Int J Clin Exp Med*. 2015;8:9403-9411.
46. Yu D, Febbo IG, Maroteaux MJ, et al. The transcription factor Shox2 shapes neuron firing properties and suppresses seizures by regulation of key ion channels in Thalamocortical neurons. *Cereb Cortex*. 2021;31:3194-3212.
47. Bischofberger J, Engel D, Li L, Geiger JR, Jonas P. Patch-clamp recording from mossy fiber terminals in hippocampal slices. *Nat Protoc*. 2006;1:2075-2081.
48. Grassi S, Tozzi A, Costa C, et al. Neural 17β-estradiol facilitates long-term potentiation in the hippocampal CA1 region. *Neuroscience*. 2011;192:67-73.
49. Bhatnagar AS, Häusler A, Schieweck K, Lang M, Bowman R. Highly selective inhibition of estrogen biosynthesis by CGS 20267, a new non-steroidal aromatase inhibitor. *J Steroid Biochem Mol Biol*. 1990;37:1021-1027.
50. Di Mauro M, Tozzi A, Calabresi P, Pettorossi VE, Grassi S. Different synaptic stimulation patterns influence the local androgenic and estrogenic neurosteroid availability triggering hippocampal synaptic plasticity in the male rat. *Eur J Neurosci*. 2017;45:499-509.
51. Di Mauro M, Tozzi A, Calabresi P, Pettorossi VE, Grassi S. Neosynthesis of estrogenic or androgenic neurosteroids determine whether long-term potentiation or depression is induced in hippocampus of male rat. *Front Cell Neurosci*. 2015;9:376.
52. Prange-Kiel J, Fester L, Zhou L, Lauke H, Carrétero J, Rune GM. Inhibition of hippocampal estrogen synthesis causes region-specific downregulation of synaptic protein expression in hippocampal neurons. *Hippocampus*. 2006;16:464-471.
53. Schulz PE, Cook EP, Johnston D. Using paired-pulse facilitation to probe the mechanisms for long-term potentiation (LTP). *J Physiol Paris*. 1995;89:3-9.
54. Xu-Friedman MA, Regehr WG. Structural contributions to short-term synaptic plasticity. *Physiol Rev*. 2004;84:69-85.
55. Zucker RS, Regehr WG. Short-term synaptic plasticity. *Annu Rev Physiol*. 2002;64:355-405.
56. Prange-Kiel J, Jarry H, Schoen M, et al. Gonadotropin-releasing hormone regulates spine density via its regulatory role in hippocampal estrogen synthesis. *J Cell Biol*. 2008;180:417-426.
57. Vierk R, Glassmeier G, Zhou L, et al. Aromatase inhibition abolishes LTP generation in female but not in male mice. *J Neurosci*. 2012;32:8116-8126.
58. Zhou L, Fester L, Haghshenas S, et al. Oestradiol-induced synapse formation in the female hippocampus: roles of oestrogen receptor subtypes. *J Neuroendocrinol*. 2014;26:439-447.
59. Brökling J, Brunne B, Rune GM. Sex-dependent responsiveness of hippocampal neurons to sex neurosteroids: a role of arc/Arg3.1. *J Neuroendocrinol*. 2022;34:e13090.
60. Brandt N, Rune GM. Sex-dependency of oestrogen-induced structural synaptic plasticity: inhibition of aromatase versus application of estradiol in rodents. *Eur J Neurosci*. 2020;52:2548-2559.
61. Grassi S, Frondaroli A, Scarduzio M, et al. Influence of sex and estrous cycle on synaptic responses of the medial vestibular nuclei in rats: role of circulating 17β-estradiol. *Brain Res Bull*. 2012;87:319-327.
62. Woolley CS, Gould E, Frankfurt M, McEwen BS. Naturally occurring fluctuation in dendritic spine density on adult hippocampal pyramidal neurons. *J Neurosci*. 1990;10:4035-4039.
63. Jain A, Huang GZ, Woolley CS. Latent sex differences in molecular signaling that underlies excitatory synaptic potentiation in the hippocampus. *J Neurosci*. 2019;39:1552-1565.
64. Kramár EA, Chen LY, Brandon NJ, et al. Cytoskeletal changes underlie Estrogen's acute effects on synaptic transmission and plasticity. *J Neurosci*. 2009;29:12982-12993.
65. Huang GZ, Woolley CS. Estradiol acutely suppresses inhibition in the hippocampus through a sex-specific endocannabinoid and mGluR dependent mechanism. *Neuron*. 2012;74:801-808.
66. Hernández-Vivanco A, Cano-Adamuz N, Sánchez-Aguilera A, et al. Sex-specific regulation of inhibition and network activity by local aromatase in the mouse hippocampus. *Nat Commun*. 2022;13:3913.
67. Topolnik L, Tamboli S. The role of inhibitory circuits in hippocampal memory processing. *Nat Rev Neurosci*. 2022;23:476-492.
68. Reddy DS. Testosterone modulation of seizure susceptibility is mediated by neurosteroids 3α-androstanediol and 17β-estradiol. *Neuroscience*. 2004;129:195-207.
69. Ubuka T, Tsutsui K. Neuropeptidergic control of neurosteroids biosynthesis. *Front Neuroendocrinol*. 2022;65:100976.
70. Tozzi A, Durante V, Manca P, et al. Bidirectional synaptic plasticity is driven by sex Neurosteroids targeting estrogen and androgen receptors in hippocampal CA1 pyramidal neurons. *Front Cell Neurosci*. 2019;13:534.
71. Fester L, Zhou L, Voets C, et al. The opposing roles of estradiol on synaptic protein expression in hippocampal cultures. *Psychoneuroendocrinology*. 2009;34(Suppl 1):S123-S129.
72. Nelson BS, Black KL, Daniel JM. Circulating estradiol regulates brain-derived estradiol via actions at GnRH receptors to impact memory in ovariectomized rats. *eNeuro*. 2016;3:ENEURO.0321-16.2016.
73. Pollard KJ, Daniel JM. Nuclear estrogen receptor activation by insulin-like growth factor-1 in neuro-2A neuroblastoma cells requires endogenous estrogen synthesis and is mediated by mutually repressive MAPK and PI3K cascades. *Mol Cell Endocrinol*. 2019;490:68-79.

How to cite this article: Maroteaux MJ, Noccioli CT, Daniel JM, Schrader LA. Rapid and local neuroestrogen synthesis supports long-term potentiation of hippocampal Schaffer collaterals-cornu ammonis 1 synapse in ovariectomized mice. *J Neuroendocrinol*. 2024;36(12):e13450. doi:10.1111/jne.13450